Inorganic Chemistry

ARTICLE

pubs.acs.org/IC

Manganese(II)-Containing MRI Contrast Agent Employing a Neutral and Non-Macrocyclic Ligand

Qiao Zhang,[†] John D. Gorden,[†] Ronald J. Beyers,[‡] and Christian R. Goldsmith[†,*]

[†]Department of Chemistry & Biochemistry, Auburn University, Auburn, Alabama 36849, United States

[‡]Auburn University Magnetic Resonance Imaging Research Center, Auburn, Alabama 36849, United States

Supporting Information

ABSTRACT: The ligand *N*,*N*′-bis(2-pyridylmethyl)-bis(ethylacetate)-1,2-ethanediamine (debpn) coordinates divalent transition metal ions in either a pentadentate or hexadentate fashion. The coordination number correlates with the ionic radius of the metal ion, with larger cations being heptacoordinate as assessed by solid-state analysis. With Mn(II), the debpn ligand is hexadentate and remains bound to the oxophilic metal ion, even when dissolved in water. The ligand's incomplete coordination of the manganous ion allows water molecules to coordinate to the metal center. These two properties, coupled with the high paramagnetism associated with the $S = 5/2$ metal center, enable $[Mn(debpn)(H_2O)](ClO_4)_2$ to serve as a stable and effective magnetic resonance imaging contrast agent despite the ligand's lack of both a macrocyclic component and an anionic charge.

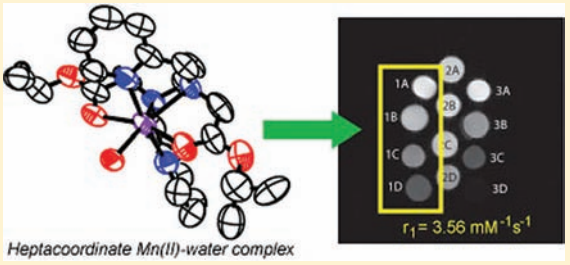

INTRODUCTION

First-row transition metal ions are commonly found with coordination numbers of four through six. Seven-coordinate transition metal complexes, conversely, are relatively rare. A 2003 survey of the Cambridge Structural Database found that heptacoordinate metal ions were found in less than 2% of the total number of structures that contained elements from Groups 3 to 12.[1] Heptacoordinate metal centers have been sought and investigated for a number of reasons. They can serve as models of intermediates in associative ligand exchange mechanisms. Their electronic structures can differ markedly from those of lower-coordinate analogs, potentially enabling novel modes of reactivity.[2]

Heptacoordinate manganous complexes, in particular, have been investigated for their potential to serve both as superoxide dismutase mimics[3−5] and as contrast agents for magnetic resonance imaging (MRI).[6−10] The latter research has the goal of developing alternatives to gadolinium-containing contrast agents. Although many Gd(III) complexes have been approved for clinical use,[11,12] there exist concerns about both their adverse effects on the human body[13,14] and the potential entrance of toxic Gd(III) species into groundwater.[15] Manganese(II) ions are attractive alternatives as the paramagnetic reporter on the bases of their high paramagnetism ($S = 5/2$) and the prevalence of manganese in biology and the environment.[16,17] In the development of clinically useful Mn(II) compounds, the use of a highly coordinating ligand is essential to maintaining the stability of the complex in aqueous solutions and regulating the metal ion's reactivity. Previously found Mn(II)-containing contrast agents, including the clinically approved Teslascan, have made use of either a macrocycle or a highly anionic ligand to further ensure aqueous stability[6,7,9] and prevent manganism in biological subjects.[18]

The shortage of stable seven-coordinate transition metal complexes hinders attempts to understand their reactivity, make comparisons to related lower-coordinate species, and develop clinically useful Mn(II) compounds. One complication is the lack of ligands that can reliably coordinate metals to this extent. Heptacoordination around first-row transition metal ions often requires a constrained ligand, such as a pentadentate macrocycle.[1,2,6,19,20] In rarer cases, hexadentate ligands may allow an additional monodentate ligand to coordinate.[21−24]

Presented are a novel ligand, *N*,*N*′-bis(2-pyridylmethyl)-bis-(ethylacetate)-1,2-ethanediamine (debpn, Scheme 1), and its complexes with divalent first-row transition metal ions. The ligand binds to Mn(II), Fe(II), and Zn(II) in a hexadentate fashion, binding through the two pyridine rings, the two amine nitrogens, and the two carbonyl groups of the esters (Scheme 1). A water molecule completes the heptacoordination around Mn(II) and Fe(II); whereas, the Zn(II) is hexacoordinate. With smaller metal ions, such as Co(II) and Ni(II), debpn behaves as a pentadentate ligand, with one of the O-donors remaining unbound. The $[Mn(debpn)(H_2O)]^{2+}$ complex appears to be stable in water. The Mn(II) compound's ability to bind water molecules and remain intact in water over several hours, despite the absence of a macrocycle and anionic donor atoms within the ligand, led us to investigate its capacity to act as a MRI contrast agent.

Received: May 6, 2011
Published: September 02, 2011

Scheme 1

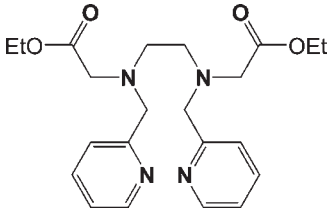

EXPERIMENTAL SECTION

Materials. 2-Pyridinecarboxaldehyde, ethyl bromoacetate, anhydrous acetonitrile (MeCN), manganese(II) perchlorate hydrate, iron(II) perchlorate hydrate, cobalt(II) perchlorate hydrate, nickel(II) perchlorate hydrate, copper(II) perchlorate hydrate, zinc(II) perchlorate hydrate, basic alumina (Brockmann I activity), silica (60 Å), potassium carbonate (K_2CO_3), sodium borohydride ($NaBH_4$), and 4-(2-hydroxyethyl)-1-piperazineethanesulfonic acid (HEPES) were purchased from Sigma-Aldrich and used as received, unless noted otherwise. Iron(II) triflate was prepared as previously described.[25] Diethyl ether (ether), ethyl acetate (EtOAc), methanol (MeOH), and potassium iodide (KI) were bought from Fisher. 1,2-Ethylenediamine, diethyl ether (ether), dichloromethane (CH_2Cl_2), and ethanol (EtOH) were purchased from Fluka, Mallinckrodt Baker, and Pharmco-AAPER, respectively. Chloroform-*d* ($CDCl_3$) and acetonitrile-d_3 (CD_3CN) were bought from Cambridge Isotopes and used as received. *N,N′*-bis(2-pyridylmethyl)-1,2-ethanediamine (bispicen) was prepared through a precedented procedure.[26]

Caution: Although no problems were encountered with the described chemistry, perchlorate salts of metal complexes are potentially explosive. The danger can be minimized by working with small quantities of these reagents and using appropriate safety measures, such as protective shields, for their preparation and handling.

Instrumentation. ^{1}H and ^{13}C NMR spectra were recorded on a 250 or 400 MHz AV Bruker NMR spectrometer at 293 K unless stated otherwise and referenced to internal standards. Elemental analyses (C, H, N) were performed by Atlantic Microlabs (Norcross, GA). All samples subjected to elemental analysis were crystallized and dried under vacuum prior to their shipment. IR spectra were collected by a Shimadzu IR Prestige-21 FT-IR spectrophotometer. Electron paramagnetic resonance (EPR) spectra were collected on a Bruker EMX-6/1 X-band EPR spectrometer operated in the perpendicular mode and analyzed with the program EasySpin. Each sample was run as a frozen solution in a quartz tube. A Johnson Matthey magnetic susceptibility balance (model MK I#7967) was used to measure the magnetic moments of solid samples. High resolution mass spectrometry (HR-MS) data were acquired at the Mass Spectrometer Center at Auburn University on a Bruker microflex LT MALDI-TOF mass spectrometer via direct probe analysis operated in the positive ion mode.

X-ray Crystallography. Crystals were mounted in paratone oil on glass fibers and aligned on a Bruker SMART APEX CCD X-ray diffractometer. Intensity measurements were performed using graphite monochromated Mo Kα radiation (λ = 0.71073 Å) from a sealed tube and monocapillary collimator. SMART (v 5.624) was used to determine the preliminary cell constants and regulate the data acquisition. The intensities of reflections of a sphere were collected through the compilation of three sets of exposures (frames). Each set had a different ϕ angle for the crystal, with each exposure spanning a range of 0.3° in ω. A total of 1800 frames were collected with exposure times of 40 s per frame. The data were corrected for Lorentz and polarization effects. Structures were solved using direct methods and expanded using Fourier techniques. All non-hydrogen atoms were refined anisotropically. Hydrogen atoms were included at idealized positions 0.95 Å from their parent atoms prior to the final refinement. Further details regarding the data acquisition and analysis are included in Table 1 and in the Supporting Information. Structural overlays were performed using the Mercury software (v. 2.4.5) available from the Cambridge Crystallographic Database Centre.

Magnetic Resonance Imaging (MRI). All MRI data were collected at the Auburn University MRI Research Center. All measurements were run on a Siemens Verio open-bore 3-T MRI clinical scanner using a 15-channel knee coil to simultaneously image 12−15 samples. An inversion recovery (IR) sequence was used that featured a non-selective adiabatic inversion pulse followed by a slice-selective gradient recalled echo (GRE) readout after a delay period corresponding to the inversion time (TI).[27,28] The GRE was a saturation readout, such that only one line of k-space was acquired per repetition time (TR), in order to maximize both signal strength and the accuracy of the T_1 estimates. The specific imaging parameters were as follows: TR was set to 4 s, TI was varied from 4.8 to 2500 ms over 37 steps, the echo time (TE) was set to 3.6 ms, the flip angle equaled 90°, averages = 1, slice thickness = 5 mm, field of view = 140 × 140 mm, matrix = 128 × 128, resulting in a pixel size of 1.1 × 1.1 × 5.0 mm. All samples were run in 50 mM solutions of HEPES in water that were buffered to pH 7.00 and kept at 22 °C. $[Mn(H_2O)_6](ClO_4)_2$, $Na_2[Mn(EDTA)(H_2O)]$, and $[Mn(debpn)(H_2O)](ClO_4)_2$ were investigated. The manganese content was systematically varied from 0.10 to 1.00 mM. The inverses of the T_1 values were plotted versus the concentration of Mn(II) to obtain r_1 values.

MRI Data Analysis. Image analysis was performed using custom Matlab programs (Mathworks, Natick, MA). The initial TI = 4.8 ms image was used as a baseline to determine circular region of interest (ROI) boundaries for each sample; from these, the mean pixel magnitudes for each ROI were calculated. For each of the 36 subsequent TI images, the same ROI boundaries were applied and the mean pixel magnitude calculations were repeated. This gave consistent ROI spatial definitions and a corresponding time course of magnitudes for each of the samples over all the TI time points. Each sample's complex phase was used to correct the magnitude polarity to produce a complete exponential T_1 inversion recovery curve. The Nelder-Mead simplex algorithm[29] was applied to each sample's exponential curve to estimate its corresponding T_1 value.

Syntheses. *N,N′-Bis(2-pyridylmethyl)-bis(ethylacetate)-1,2-ethanediamine (debpn).* Ethyl bromoacetate (3.34 g, 20.0 mmol), K_2CO_3 (2.76 g, 20.0 mmol), and KI (3.32 g, 20.0 mmol) were added to a solution of bispicen (2.42 g, 10.0 mmol) in 20 mL of anhydrous MeCN. The resultant mixture was stirred under N_2 for 48 h at room temperature. After this period, the solution was filtered to remove inorganic salts, and the filtrate was concentrated to a brown oil under reduced pressure. The product was purified through column chromatography. The crude material was run first on a basic alumina support, using CH_2Cl_2 as an elutant, then a silica support with a 10:1 EtOAc/EtOH solution as the elutant (R_f = 0.47). The product is isolated as a yellow oil (1.10 g, 31%). ^{1}H NMR (250 MHz, $CDCl_3$): δ 1.23 (t, 3H, OCH_2CH_3), 2.84 (s, 2H, NCH_2CH_2N), 3.42 (s, 2H, NCH_2-Py), 3.92 (s, 2H, NCH_2CO_2Et), 4.13 (q, 2H, OCH_2CH_3), 7.12 (t, 1H, 5-Py*H*), 7.46 (d, 1H, 3-Py*H*), 7.61 (t, 1H, 4-Py*H*), 8.51 (d, 1H, 6-Py*H*). ^{13}C NMR (62.5 MHz, $CDCl_3$): δ 14.1, 52.1, 54.5, 60.3, 60.5, 121.9, 123.0, 136.4, 149.0, 159.5, 171.4. IR (KBr, cm^{-1}): 3052 (w), 2982 (m), 2937 (m), 2908 (m), 2847 (m), 2374 (w), 2318 (w), 2276 (w), 1738 (s, C═O), 1729 (s, C═O), 1590 (s), 1570 (m), 1475 (s), 1434 (s), 1370 (s), 1299 (m), 1260 (s), 1191 (s), 1029 (s), 995 (m), 761 (s). MS (ESI): Calcd for MH^+, 415.2345; Found, 415.2343.

Aqua(N,N′-bis(2-pyridylmethyl)-bis(ethylacetate)-1,2-ethanediamine) manganese(II) Perchlorate ([Mn(debpn)(H$_2$O)](ClO$_4$)$_2$). An anaerobic solution of debpn (0.830 g, 2.00 mmol) in 5.0 mL of anhydrous MeCN

dx.doi.org/10.1021/ic2009495 |*Inorg. Chem.* 2011, 50, 9365–9373

Table 1. Selected Crystallographic Data for Coordination Complexes[a]

parameter	[Mn(debpn)(H_2O)] (ClO_4)$_2$	[Fe(debpn)(H_2O)] (CF_3SO_3)$_2$)	[Co(debpn)(MeCN)] (ClO_4)$_2$	[Ni(debpn)(MeCN)] (ClO_4)$_2$	[Zn(debpn)] (ClO4)$_2$
formula	$C_{22}H_{32}Cl_2MnN_4O_{13}$	$C_{24}H_{32}F_6FeN_4O_6S_6$	$C_{24}H_{33}Cl_2CoN_5O_{12}$	$C_{24}H_{33}Cl_2N_5NiO_{12}$	$C_{22}H_{30}Cl_2N_4O_{12}Zn$
MW	686.36	754.45	713.38	713.16	678.77
cryst syst	monoclinic	orthorhombic	triclinic	triclinic	monoclinic
space group	*C2/c (#15)*	*Fdd2 (#43)*	*P$\bar{1}$(#2)*	*P$\bar{1}$(#2) (#2)*	*C2/c (#15)*
a (Å)	13.5732(10)	13.983(2)	10.2626(6)	10.3714(7)	15.7195(14)
b (Å)	9.5786(10)	47.723(8)	12.7750(8)	12.6946(9)	13.5426(12)
c (Å)	22.716(2)	9.4858(15)	13.5173(8)	13.5156(10)	13.0717(12)
α (deg)	90	90	72.270(1)	71.807(2)	90
β (deg)	99.247(3)	90	70.608(1)	70.823(2)	100.910(2)
γ (deg)	90	90	73.394(1)	73.280(2)	90
V (Å^3)	2915.0(5)	6330.1(18)	1558.25(16)	1562.35(19)	2732.4(4)
Z	4	8	2	2	4
cryst color	colorless	yellow	orange	purple	white
T (K)	193(2)	198(2)	193(2)	193(2)	198(2)
reflns collected	11666	15823	15863	16017	13634
unique reflns	3597	3390	7617	4364	2336
$R1$ (F, $I > 2\sigma(I)$)	0.0518	0.0409	0.0577	0.0705	0.080
w$R2$ (F^2, all data)	0.1589	0.0998	0.1847	0.1976	0.1901

[a] $R1 = \Sigma||F_o| - |F_c||/\Sigma|F_o|$; $wR2 = [\Sigma w(F_o^2 - F_c^2)^2/\Sigma wF_o^4]^{1/2}$.

was added to 0.506 g of $Mn(ClO_4)_2$ (1.86 mmol). The mixture stirred under N_2 for 60 min, yielding a yellow solution. At the end of the 60 min, 15 mL of ether was added to precipitate the product as pale yellow crystals suitable for single crystal X-ray diffraction (0.69 g, 52%). Solid-state magnetic susceptibility (295 K): μ_{eff} = 6.1 μ_B. EPR (H_2O, 77 K, X-band): g_{eff} = 6.07, 3.28, 2.00. IR (KBr, cm^{-1}): 2953 (w), 2915 (w), 2903 (w), 2360 (w), 2344 (w), 1729 (w), 1678 (s, C═O), 1645 (w, C═O), 1605 (m, C═O), 1571 (w), 1434 (m), 1410 (m), 1387 (m), 1321 (m), 1302 (m), 1277 (w), 1239 (m), 1161 (m), 1115 (s), 1101 (s), 1059 (s), 1015 (m), 1000 (m), 990 (w), 947 (m), 932 (w), 867 (w), 834 (m), 770 (m), 732 (m), 622 (s). Elemental Analysis: Calcd for $C_{22}H_{32}N_4O_{13}MnCl_2$: C, 38.50; H, 4.70; N, 8.16; Found: C, 38.46; H, 4.63; N, 7.67.

Aqua(N,N′-bis(2-pyridylmethyl)-bis(ethylacetate)-1,2-ethanediamine) iron(II) Perchlorate ([Fe(debpn)(H_2O)](ClO_4)$_2$). An anaerobic solution of debpn (0.830 g, 2.00 mmol) in 5.0 mL of anhydrous MeCN was added to 0.508 g iron(II) perchlorate hydrate (1.86 mmol). The mixture was stirred under an anaerobic atmosphere for 60 min. At the end of this time, 15 mL of ether was added to the brown solution to precipitate the product as a brownish yellow microcrystalline powder (1.13 g, 85%). Crystals suitable for single-crystal X-ray diffraction were grown from saturated solutions of the triflate analog in MeCN. The following measurements pertain to the perchlorate complex. Solid-state magnetic susceptibility (295 K): μ_{eff} = 4.7 μ_B. Optical spectroscopy (MeCN): 260 nm (8000 M^{-1} cm^{-1}), 343 nm (1000 M^{-1} cm^{-1}). IR (KBr, cm^{-1}): 2986 (w), 2958 (w), 2911 (w), 2873 (w), 2362 (w), 2331 (w), 1673 (s, C═O), 1644 (m, C═O), 1608 (m, C═O), 1572 (w), 1479 (w), 1443 (m), 1422 (m), 1488 (m), 1360 (w), 1322 (m), 1285 (s), 1249 (s), 1225 (s), 1171 (s), 1160 (s), 1138 (s), 1029 (s), 1004 (w), 990 (w), 948 (m), 871 (w), 840 (m), 772 (m), 758 (m), 729 (m), 640 (s). Elemental Analysis: Calcd for $C_{22}H_{32}N_4O_{13}FeCl_2$: C, 38.45; H, 4.69; N, 8.15; Found: C, 37.87; H, 4.53; N, 8.03.

Acetonitrilo(N,N′-bis(2-pyridylmethyl)-bis(ethylacetate)-1,2-ethanediamine)cobalt(II) Perchlorate ([Co(debpn)(MeCN)](ClO$_4$)$_2$). An anaerobic solution of debpn (0.414 g, 1.00 mmol) in 5.0 mL of anhydrous MeCN was added to 0.366 g of $Co(ClO_4)_2 \cdot 6H_2O$ (1.00 mmol). The mixture stirred under N_2 for 60 min, yielding a red solution. At the end of the 60 min, 15 mL of ether was added to precipitate the product as red crystals suitable for single crystal X-ray diffraction (0.300 g, 42%). Solid-state magnetic susceptibility (295 K): μ_{eff} = 4.0 μ_B. Optical spectroscopy (MeCN): 475 nm (45 M^{-1} cm^{-1}). IR (KBr, cm^{-1}): 2987 (w), 2959 (w), 2938 (w), 2359 (w), 2343 (w), 2331 (w), 2284 (w), 2016 (w), 1733 (s, C═O), 1666 (s, C═O), 1609 (m, C═O), 1414 (w), 1382 (w), 1355 (w), 1344 (w), 1306 (m), 1292 (m), 1262 (m), 1211 (s), 1162 (w), 1092 (s), 1019 (m), 996 (w), 953 (w), 878 (w), 843 (w), 822 (w), 797 (w), 768 (m), 734 (w), 718 (w), 648 (w), 623 (s). Elemental Analysis: Calcd for $C_{24}H_{33}N_5O_{12}CoCl_2$: C, 40.41; H, 4.66; N, 9.82; Found: C, 39.95; H, 4.58; N, 9.64.

Acetonitrilo(N,N′-bis(2-pyridylmethyl)-bis(ethylacetate)-1,2-ethanediamine)nickel(II) Perchlorate ([Ni(debpn)(MeCN)](ClO$_4$)$_2$). The ligand debpn (0.144 g, 0.348 mmol) was put under nitrogen and dissolved in 5.0 mL of anhydrous MeCN. This solution was added to 0.110 g of $Ni(ClO_4)_2 \cdot 6H_2O$ (0.300 mmol). The resultant purple solution stirred under N_2 for 60 min. The product crystallized as a purple solid (0.119 g, 56%) upon the addition of 15 mL of ether. These crystals were suitable for X-ray diffraction. Solid-state magnetic susceptibility (295 K): μ_{eff} = 2.8 μ_B. Optical spectroscopy (MeCN): 550 nm (16 M^{-1} cm^{-1}), 890 nm (17 M^{-1} cm^{-1}). IR (KBr, cm^{-1}): 2988 (w),2964 (w), 2938 (w), 2314 (w), 2286 (w), 2016 (w), 1737 (s, C═O), 1668 (s, C═O), 1610 (m, C═O), 1429 (m), 1414 (w), 1381 (w), 1355 (w), 1343 (w), 1290 (w), 1262 (w), 1210 (m), 1093 (s), 1059 (m), 1022 (m), 998 (w), 939 (w), 881 (w), 840 (w), 824 (w), 799 (w), 776 (m), 767 (m), 734 (w), 718 (w), 666 (w), 623 (s). Elemental Analysis: Calcd for $C_{24}H_{33}N_5O_{12}NiCl_2$: C, 40.42; H, 4.66; N, 9.82; Found: C, 39.93; H, 4.64; N, 9.64.

(N,N′-bis(2-pyridylmethyl)-bis(ethylacetate)-1,2-ethanediamine) zinc(II) Perchlorate ([Zn(debpn)](ClO$_4$)$_2$). An anaerobic solution of debpn (0.124 g, 0.300 mmol) in 5.0 mL of anhydrous MeCN was added to 0.112 g of $Zn(ClO_4)_2 \cdot 6H_2O$ (0.300 mmol). The pale yellow mixture stirred under N_2 for 60 min. The product crystallized as pale yellow crystals (0.145 g, 69%) upon the addition of 15 mL of ether. These crystals were suitable for X-ray diffraction. IR (KBr, cm^{-1}): 2987 (w), 2979 (w), 2939 (w), 2876 (w), 2361 (w), 2340 (w), 2253 (w), 2021 (w),

dx.doi.org/10.1021/ic2009495 |*Inorg. Chem.* 2011, 50, 9365–9373

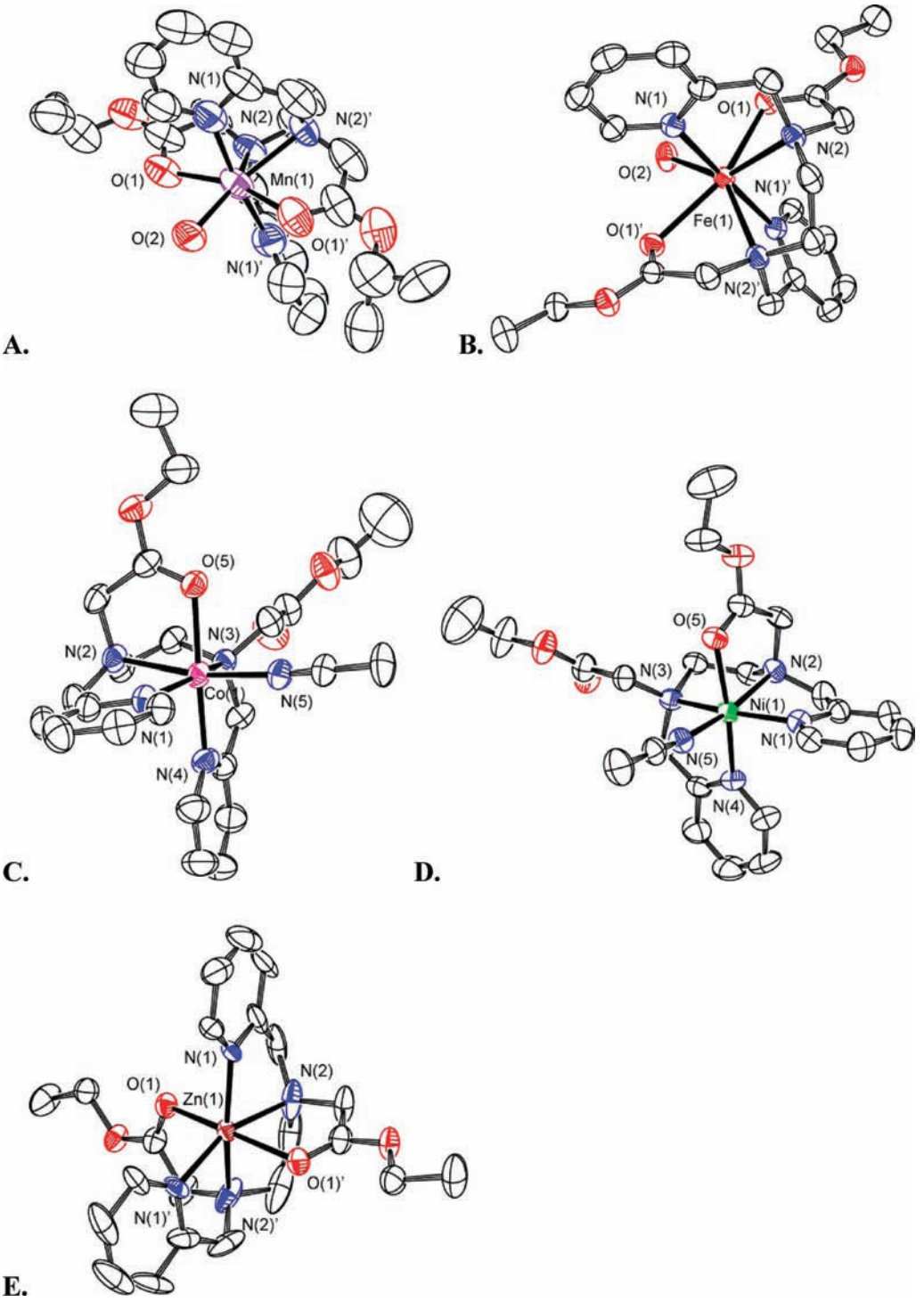

Figure 1. ORTEP representations of the dications (A) $[Mn(debpn)(H_2O)]^{2+}$, (B) $[Fe(debpn)(H_2O)]^{2+}$, (C) $[Co(debpn)(MeCN)]^{2+}$, (D) $[Ni(debpn)(MeCN)]^{2+}$ and (E) $[Zn(debpn)]^{2+}$. All hydrogen atoms, counterions, and noncoordinated solvent molecules have been removed for clarity. All thermal ellipsoids are drawn at 50% probability.

1738 (w), 1733 (w), 1673 (s, C═O), 1613 (s, C═O), 1488 (m), 1464 (m), 1447 (s), 1435 (s), 1398 (m), 1374 (s), 1347 (m), 1310 (m), 1284 (m), 1264 (s), 1162 (m), 1093 (s), 1028 (s), 1012 (s), 995 (s), 970 (m), 953 (m), 936 (m), 898 (w), 871 (m), 841 (m), 830 (w), 817 (m), 764 (s), 745 (w), 730 (w), 668 (w), 651 (m), 601 (s). Elemental Analysis: Calcd for $C_{22}H_{30}N_4O_{12}ZnCl_2 \bullet H_2O$: C, 37.92; H, 4.63; N, 8.04; Found: C, 37.45; H, 4.54; N, 8.10.

RESULTS

Syntheses. The ligand is prepared in moderate yield in two steps from commercially available reagents. The preparation of the metal complexes is straightforward, with yields ranging from 52% to 85%. Attempts to prepare a Cu (II) complex yielded a blue crystalline material which did not diffract X-ray radiation.

Table 2. Comparison of the Bond Lengths (Å) and Bond Angles (deg) for the Heptacoordinate Complexes $[Mn(debpn)(H_2O)]^{2+}$ and $[Fe(debpn)(H_2O)]^{2+}$[a]

bond length	Mn	Fe	angle	Mn	Fe
			N(1)−M−N(1)′	172.33(15)	176.68(13)
M−O(1)	2.374(3)	2.2946(19)	O(1)−M−N(1)′	98.73(10)	95.70(7)
M−O(2)	2.159(3)	2.184(3)	O(1)−M−N(2)	68.58(10)	69.70(8)
M−N(1)	2.260(3)	2.204(2)	O(1)−M−N(2)′	130.57(11)	134.27(8)
M−N(2)	2.371(3)	2.322(2)	O(2)−M−N(1)	93.84(7)	91.66(7)
angle	Mn	Fe	O(2)−M−N(2)	142.28(8)	142.05(6)
O(1)−M−O(1)′	159.23(13)	154.27(11)	N(1)−M−N(2)	101.42(11)	103.07(8)
O(1)−M−O(2)	79.61(6)	77.14(5)	N(1)−M−N(2)′	72.31(12)	74.22(8)
O(1)−M−N(1)	82.67(11)	85.05(7)	N(2)−M−N(2)′	75.43(15)	75.91(11)

[a] Note that the ligands' donor atoms from the CIF files have been relabeled in accordance with Figure 1 in order to facilitate comparison of the structures.

Table 3. Comparison of the Bond Lengths (Å) and Bond Angles (deg) for the Hexacoordinate Complexes $[Co(debpn)(MeCN)]^{2+}$ and $[Ni(debpn)(MeCN)]^{2+}$[a]

bond length	Co	Ni	angle	Co	Ni
M−N(1)	2.208(2)	2.088(4)	N(1)−M−O(5)	90.41(9)	94.70(14)
M−N(2)	2.161(2)	2.097(4)	N(2)−M−N(3)	78.58(10)	84.53(14)
M−N(3)	2.112(2)	2.169(4)	N(2)−M−N(4)	97.38(10)	97.26(15)
M−N(4)	2.116(3)	2.062(4)	N(2)−M−N(5)	168.29(10)	168.64(15)
M−N(5)	2.073(2)	2.044(4)	N(2)−M−O(5)	80.00(9)	81.64(14)
M−O(5)	2.098(2)	2.086(4)	N(3)−M−N(4)	91.96(10)	81.22(15)
angle	Co	Ni	N(3)−M−N(5)	99.61(10)	98.08(14)
N(1)−M−N(2)	83.40(9)	80.07(15)	N(3)−M−O(5)	97.42(9)	90.56(13)
N(1)−M−N(3)	158.73(9)	162.80(14)	N(4)−M−N(5)	94.23(10)	94.07(16)
N(1)−M−N(4)	79.18(10)	93.12(15)	N(4)−M−O(5)	169.52(9)	171.78(14)
N(1)−M−N(5)	100.29(9)	98.51(15)	N(5)−M−O(5)	88.82(9)	87.26(14)

[a] Note that the ligands' donor atoms in the CIF files have been relabeled in accordance with Figure 1 in order to facilitate comparison of the structures.

The elemental analysis of the copper compound was not consistent with $[Cu(debpn)(X)](ClO_4)_2$ with X = MeCN, H_2O, or null. Due to the ambiguity of its composition, the copper compound will not be discussed further in this work.

Structural Characterization. The M(II) complexes with debpn crystallize from saturated MeCN solutions upon cooling or the addition of ether. In each case, the cations contain mononuclear metal centers with a 1:1 ratio of ligand to metal. The wR^2 values (Table 1) are relatively high due to disorder in both the ester groups of the debpn ligand and the perchlorate anions.

The Mn(II) and Fe(II) compounds contain heptacoordinate metal ions (Figure 1A,B). The debpn ligand coordinates through six atoms: the four nitrogen atoms from the pyridine rings and the tertiary amines and the two carbonyl oxygen atoms from the pendant esters. Although the crystals are grown in MeCN, a molecule of H_2O completes the coordination around each of these two metal ions. The source of the water is likely the perchlorate salt. The coordination around each is best described as a distorted pentagonal bipyramid, as assessed by the L−M−L bond angles, with the pyridine rings occupying the axial positions (Table 2). On the basis of a least-squares analysis of the L−M−L bond angles, the Fe(II) complex appears to have the less distorted geometry. The N-donors coordinate the metal ions in a distorted *cis*-α conformation, with the amine nitrogens closer together than in their hexacoordinate analogs.[30] As anticipated, the M−L bond distances are shorter for the Fe(II) complex.[31]

Table 4. Bond lengths (Å) and Bond Angles (deg) for $[Zn(debpn)]^{2+}$

bond length	Zn	angle	Zn
M−N(1)	2.063(4)	N(1)−M−N(1)′	119.8(2)
M−N(2)	2.173(5)	N(1)−M−N(2)′	159.0(2)
M−O(1)	2.201	N(1)−M−O(1)′	90.12(14)
		N(2)−M−O(1)	78.63(15)
angle	Zn	N(2)−M−N(2)′	83.8(3)
N(1)−M−N(2)	79.2(2)	N(2)−M−O(1)′	93.52(15)
N(1)−M−O(1)	95.13(14)	O(1)−M−O(1)′	169.54(17)

In the structures of the Co(II) and Ni(II) compounds (Figure 1, C and D), the metal ions are hexacoordinate, with the debpn ligand providing five donor atoms and an MeCN molecule completing the octahedral geometry. On the basis of the L−M−L bonds, the Ni(II) complex more closely approximates an ideal octahedron. The debpn ligates the metals through the four N-donors and one of the ester's carbonyl oxygen atoms. The pyridine rings are *cis* to each other (Table 3), and the coordination of the N-donors resembles the *cis*-β conformation occasionally found for tetradentate ligands with reduced imine linkages.[32,33] As anticipated, the M−L bond distances are shorter for the Ni(II) complex.[31] These average 2.09 Å, whereas, those for the Co(II) complex average 2.13 Å.

dx.doi.org/10.1021/ic2009495 |*Inorg. Chem.* 2011, 50, 9365–9373

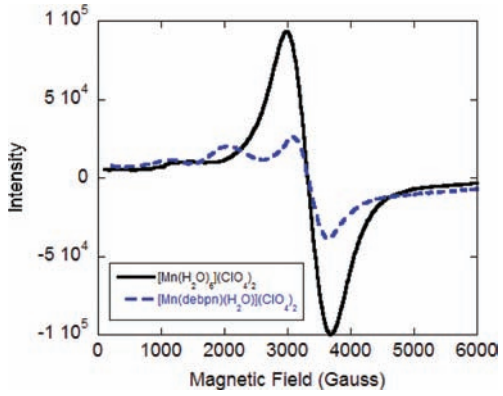

Figure 2. X-Band electron paramagnetic resonance spectra of $[Mn(H_2O)_6](ClO_4)_2$ (black) and $[Mn(debpn)(H_2O)](ClO_4)_2$ (blue) in H_2O at 77 K. The concentration of each sample is 1.0 mM. For the debpn complex, the g_{eff} values =6.07, 3.28, and 2.00. For $[Mn(H_2O)_6]^{2+}$, the g value =2.03.

Table 5. Carbonyl Stretching Frequencies for Debpn Species[a]

species	carbonyl stretches (cm^{-1})
debpn	1738, 1729
$[Mn(debpn)(H_2O)]^{2+}$	1678, 1645, 1605[b]
$[Fe(debpn)(H_2O)]^{2+}$	1673, 1644, 1608
$[Co(debpn)(MeCN)]^{2+}$	1733, 1666, 1609
$[Ni(debpn)(MeCN)]^{2+}$	1737, 1668, 1610
$[Zn(debpn)]^{2+}$	1673, 1613[c]

[a] All samples were prepared as KBr pellets. [b] Additional weak band at 1729 cm^{-1}. [c] Additional weak bands at 1738 and 1733 cm^{-1}.

In the structure of the Zn(II) complex (Figure 1, E), the metal ion is hexacoordinate, with the debpn ligand providing all six donor atoms. The esters of the ligand coordinate *trans* to each other; the four N-donors are roughly coplanar. Of the three hexacoordinate metal centers, the Zn(II) complex displays the greatest distortions from an ideal octahedral geometry, as assessed by a least-squares analysis of the L−M−L bond angles (Tables 3 and 4). The average of the M−L bond distances, 2.15 Å, is greater than those measured for the Co(II) and Ni(II) complexes.

Solution Characterization. The metal complexes with debpn were analyzed by EPR, NMR, and optical spectroscopy. The EPR spectrum of the Mn(II) complex in water (Figure 2) resembles those of other Mn(II) complexes with N-donor ligands.[32,34−36] Zero-field splitting gives rise to three features with g_{eff} = 6.07, 3.28, and 2.00. Under the conditions used to acquire the spectrum, we cannot resolve the hyperfine interactions anticipated for a nucleus with I = 5/2. The UV/vis spectrum of the Fe(II) compound resembles other heptacoordinate Fe(II) species, with a relatively low intensity LMCT band in the 300−400 nm region.[37] The spectrophotometric features of both the Co(II) and Ni(II) complexes are consistent with octahedrally coordinated metal ions,[38,39] suggesting that the hexacoordination observed in the solid-state is largely preserved in solution. The ^{1}H NMR spectrum of the Zn(II) crystals in CD_3CN defies simple explanation and appears to contain at least four diamagnetic species at room temperature, as assessed by the number of ester CH_3 peaks. Upon warming the sample from 25 to 65 °C (Figure S1 of the Supporting Information, SI), the peaks broaden and begin to coalesce. The ^{1}H NMR spectrum of the Ni(II) undergoes similar changes over this range in temperature, albeit with fewer visible resonances due to the paramagnetism of the sample (Figure S2 of the SI). The only conclusions that we can definitively draw from these data are that the solid-state structures are not exclusively maintained in solution and that the coordination of the debpn ligand to the metal ions is not static.

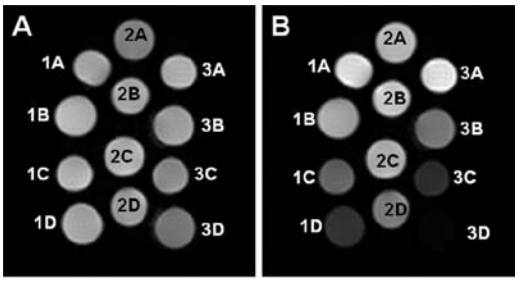

Figure 3. Inversion recovery magnetic resonance images of samples at initial time of inversion (TI) = 4.8 ms (Panel A) and TI = 160 ms (Panel B), exemplifying the different T_1 relaxation rates by the contrast change. The images with TI = 4.8 ms occur almost immediately after inversion. In the TI = 160 ms images, the more quickly relaxing samples are approaching their T_1 minima and appear darker as a consequence. Samples contained Mn(II) complexes in 50 mM HEPES solutions buffered to pH 7.00. Samples 1A-D contained $[Mn(debpn)(H_2O)](ClO_4)_2$, samples 2A-D contained $Na_2[Mn(EDTA)(H_2O)]$, and samples 3A-D contained $[Mn(H_2O)_6](ClO_4)_2$. The concentrations of the Mn(II) in the samples included: 0.10 mM (A), 0.40 mM (B), 0.70 mM (C), and 1.00 mM (D).

Solid-State Characterization. The magnetic susceptibility of each debpn complex was measured in the solid state at 295 K. The Mn(II), Fe(II), and Co(II) have μ_{eff} values consistent with high-spin d^5, d^6, and d^7 metal ions, respectively. These assignments are consistent with the aforementioned structural and spectroscopic data. The 2.8 μ_B value for $[Ni(debpn)(MeCN)]^{2+}$ is consistent with an octahedrally coordinated d^8 metal ion. The $[Zn(debpn)]^{2+}$ complex is diamagnetic, as anticipated.

The debpn ligand and its five metal complexes were also analyzed by infrared spectroscopy (IR), with a focus on the carbonyl stretching frequencies. The assigned ester C═O stretches are listed in Table 5. The frequencies of the C═O stretches for the debpn ligand (1738 cm^{-1}, 1729 cm^{-1}) are typical for organic esters. When the esters bind to the metal ion, their stretching frequencies decrease to values ranging from 1600 to 1675 cm^{-1}. The two complexes which contain nonbound esters, $[Co(debpn)(MeCN)]^{2+}$ and $[Ni(debpn)(MeCN)]^{2+}$, retain IR stretches in the 1725−1740 cm^{-1} region. The Mn(II) and the Zn(II) complexes also have weak bands in this region, which may indicate partial dissociation of the esters within the KBr pellets.

MRI Measurements. The magnetic properties of the $[Mn(debpn)(H_2O)]^{2+}$ complex were further analyzed, with a particular focus on the relaxation time of the ^{1}H nuclei of the bulk water molecules. T_1 values for different concentrations of the Mn(II) species in a 50 mM solution of HEPES buffered to pH 7.0 were obtained with the aid of a 3 T MRI instrument (Figure 3) at 22 °C. The inverses of these T_1 values were plotted as a function of $[Mn(debpn)(H_2O)]^{2+}$ concentration to obtain an r_1 value, which was subsequently compared to those measured for

dx.doi.org/10.1021/ic2009495 |*Inorg. Chem.* 2011, 50, 9365–9373

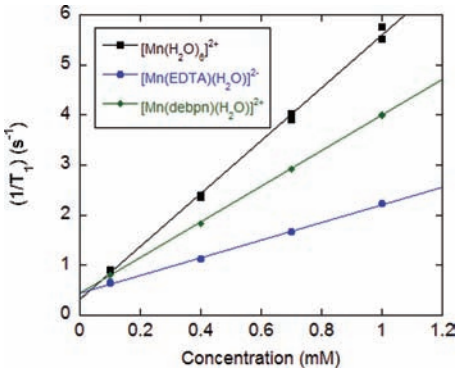

Figure 4. Plots of $(1/T_1)$ as functions of Mn(II) concentration for $[Mn(H_2O)_6](ClO_4)_2$, $Na_2[Mn(EDTA)(H_2O)]$, and $[Mn(debpn)(H_2O)](ClO_4)_2$. The shown data were collected from two sets of independently prepared samples and fit to the following equations: $[Mn(H_2O)_6]^{2+}$, $y = 0.32834 + 5.258x$ ($R = 0.99893$); $[Mn(EDTA)(H_2O)]^{2-}$, $y = 0.45333 + 1.7607x$ ($R = 0.99914$); $[Mn(debpn)(H_2O)]^{2+}$, $y = 0.43613 + 3.5573x$ ($R = 0.9999$).

$[Mn(H_2O)_6](ClO_4)_2$ and $Na_2[Mn(EDTA)(H_2O)]$ (Figure 4) under the same conditions. The numbers of water molecules in the coordination spheres of these latter two manganous species are well established as $q = 6$ and $q = 1$, respectively.[6,8,10] Comparison of the r_1 values of the three Mn(II) compounds serves two goals. First, it can confirm that the debpn ligand remains bound to the metal in aqueous solution. Second, it can potentially assess whether additional equivalents of water are displacing portions of the debpn ligand, which is more weakly bound to the metal ion than the EDTA ligand on account of its charge neutrality.

The r_1 value for the $[Mn(debpn)(H_2O)]^{2+}$ complex was found to be 3.56 ($\pm$0.14) $mM^{-1}\ s^{-1}$. As anticipated, this is less than the 5.26 ($\pm$0.21) $mM^{-1}\ s^{-1}$ value for $[Mn(H_2O)_6]^{2+}$. This r_1 value, however, is greater than the 1.76 ($\pm$0.07) $mM^{-1}\ s^{-1}$ value we measured for the other monoaqua species, $[Mn(EDTA)(H_2O)]^{2-}$. The measured r_1 values for $[Mn(H_2O)_6]^{2+}$ and $[Mn(EDTA)(H_2O)]^{2-}$ are similar but not identical to those that had been previously measured at 90 MHz and 37 °C.[8,40] Discrepancies between our values and the previously reported ones are anticipated, given the different solution media, temperature, and magnetic field strength used in the prior work.[8] The linearity of the $1/T_1$ plot over concentrations ranging from 0.1 to 1.0 mM suggests that the debpn ligand remains associated with the Mn(II) ion over these concentrations. If a significant percentage of the complexes were to fully dissociate in solution, then the r_1 value should more closely approximate that of the $[Mn(H_2O)_6]^{2+}$ species at lower concentrations, resulting in a curved plot. The T_1 values associated with each concentration of $[Mn(debpn)(H_2O)]^{2+}$ remained constant over a 15 h period, providing a lower limit of the complex's stability. Mass spectrometry of the debpn ligand after this 15 h period confirmed that the ligand remained intact, with no hydrolysis of its ester groups.

DISCUSSION

Structural analyses of ligands that encourage heptacoordination are rare; in most instances, only certain complexes within a series are structurally characterized, which limits systematic analysis of the ligand's binding tendencies.[2,21]

The ligand *N*,*N*′-bis(2-pyridylmethyl)-bis(ethylacetate)-1,2-ethanediamine (debpn) can be made in two steps from commercially available chemicals. The only complication is that two sequential chromatography columns are needed to purify the product at the end of the second step. Although the yield is modest (30%), multigram quantities of debpn can be made relatively quickly. One attractive feature of the synthesis is that it should be readily modifiable. A wide array of diamine backbones and esters could be substituted without necessitating drastic changes in the general procedure. The debpn ligand readily forms complexes with divalent first-row transition metal ions, with yields of crystalline material ranging from moderate (42%, cobalt) to excellent (85%, iron). In each case, the isolated product is a mononuclear species with a 1:1 ligand/metal ratio. The composition and structure of an isolated Cu(II) complex with debpn were never assigned with certainty.

The largest metal ions, Mn(II) and Fe(II), are heptacoordinate when bound to debpn; whereas, the others are hexacoordinate. The donor atoms in the heptacoordinate complexes are arrayed in distorted pentagonal bipyramidal geometries that are nearly isostructural. A structural overlay of the seven donor atoms and the metal center from the two complexes yields a rms value of 0.0775 $Å^{-1}$. According to a least-squares analysis of the L−M−L bond angles, the Fe(II) complex is slightly less distorted from the ideal pentagonal bipyramid. The analysis suggests that the distortions arise largely from the positions of the ester oxygen atoms and the amine nitrogen atoms. The N(1)−M−N(2)′, O(1)−M−N(2)′, and O(1)−M−O(1)′ bond angles are farthest from their idealized values (90°, 144°, and 144°), with greater digressions observed for $[Mn(debpn)(H_2O)]^{2+}$ (Table 2).

Among the hexacoordinate complexes, $[Ni(debpn)(MeCN)]^{2+}$ has its donor atoms arrayed in the closest approximation of an ideal octahedral geometry, as assessed by a least-squares analysis of the L−M−L bond angles. Under the same criteria, the Zn(II) complex is the most distorted, in large part due to the 119.8° N(1)−Zn-N(1)′ bond angles. Given that Zn(II), as a d^{10} metal ion, has no strong electronic structural preferences, it may be anticipated to better tolerate deviations from octahedral coordination. The Co(II) complex more closely resembles the Ni(II) than the Zn(II) with respect to the composition of its coordination sphere, the relative orientation of the ligand's donor atoms, and its approximation of an ideal octahedral geometry. The M−N bonds for these three compounds have lengths similar to those found in other M(II) complexes with sterically encumbered bispicen ligands.[41,42]

The mode of debpn coordination is strongly linked to the size of the metal ion, with a predisposition to bind smaller metal ions in an octahedral fashion. When the metal ion is too large, overall pentagonal bipyramidal geometries ensue. Although Co(II) is electronically compatible with heptacoordination, unlike Ni(II),[2] its ionic radius appears to be too small to accommodate all seven of the donor atoms from this particular ligand. The structures of the debpn complexes are reminiscent of the coordinative behavior of ethylenediaminetetraacetate (EDTA), which forms heptacoordinate complexes with Fe(II) and Mn(II) but hexacoordinate complexes with Ni(II) and Co(II).[4,23,43]

The coordination of ester carbonyl groups to metal ions is unusual, but precedented, in nonorganometallic coordination chemistry. The $M-O_{ester}$ bond distances in the debpn complexes are similar to those previously reported for metal-ester complexes with comparable coordination numbers, oxidation numbers, and spin-states.[37,44−49] The M−O bond distances for

dx.doi.org/10.1021/ic2009495 |*Inorg. Chem.* 2011, 50, 9365–9373

$[Co(debpn)(MeCN)]^{2+}$ and $[Ni(debpn)(MeCN)]^{2+}$ are among the shortest measured for nonorganometallic Co(II) and Ni(II) complexes with ester O-donors.[46−49] Upon coordination of the ester to the metal ion, the C═O stretches decrease (Table 5), analogous to what has been observed for CO chemistry.[50] The seven-coordinate complexes each contain an additional C═O band around 1645 cm^{-1}, but otherwise, the frequencies of the metal-bound ester C═O stretches remain relatively constant throughout the series.

The ^1H NMR spectrum of the Zn(II) complex is inconsistent with the solid-state structure, since it displays many more resonance peaks than anticipated from the complex's C_2 symmetry (Figure S1 of the SI). Upon heating the solution sample, these resonances broaden and begin to coalesce. The variable temperature data suggest that the coordination of the debpn ligand is both flexible and dynamic, with the flexibility being anticipated from the structural data. The exact Zn(II) species in solution cannot be assigned with certainty. These may include stereoisomers of the solid-state structure with the N-donors of the debpn ligand in a *cis*-α or *cis*-β conformation around the Zn(II) center. These conformers may exchange with each other through either partial, temporary ligand dissociation or Bailar or Ray-Dutt twists. Other reasonable possibilities for the additional species in solution include higher-coordinate complexes such as $[Zn(\kappa\text{-}6\text{-debpn})(MeCN)]^{2+}$, which would be analogous to the Fe(II) and Mn(II) complexes. Alternatively, the esters could be displaced by solvent molecules to yield species such as $[Zn(\kappa\text{-}5\text{-debpn})(MeCN)]^{2+}$, analogous to the Co(II) and Ni(II) complexes. The ^1H NMR spectrum of the Ni(II) complex undergoes similar changes upon heating (Figure S2 of the SI), and we speculate that similar speciation likely occurs for the other metal complexes.

The EPR spectrum of the Mn(II) complex in H_2O is distinct than that for $[Mn(H_2O)_6]^{2+}$ (Figure 2). This suggests that the debpn ligand remains at least mostly coordinated to the metal ion in aqueous solution. On the basis of the NMR data for the other metal complexes, we believe that it is unlikely that the solid-state structure is exclusively maintained in water. Spectroscopic analysis found no signs of metal dissociation or ligand decomposition over 15 h. The aqueous stability and the presence of the bound water molecule in the crystal structure prompted us to investigate $[Mn(debpn)(H_2O)]^{2+}$ as a potential contrast agent for magnetic resonance imaging. The measurements were performed on aqueous solutions of the Mn(II) compounds buffered to pH 7.00 and used a 3 T MRI scanner that is also used for clinical purposes. Comparison of the r_1 value to that of $[Mn(H_2O)_6](ClO_4)_2$ corroborates the aqueous stability of the Mn-debpn adduct, which should and does have a lower r_1 on the basis of its fewer coordinated molecules of water (q). The r_1 value is greater than our measured value for $[Mn(EDTA)(H_2O)]^{2-}$, despite the ostensibly equal q values.

Three explanations may rationalize this difference. First, additional water molecules may be coordinating to the Mn(II) in $[Mn(debpn)(H_2O)]^{2+}$. The ester groups, as seen in the crystal structures of the Co(II) and Ni(II) complexes with debpn, are relatively easy to detach from the divalent metal ions. The anionic carboxylate groups of the EDTA ligand are more difficult to displace, and the deprotonated EDTA ligand binds much more strongly to Mn(II) than debpn as assessed by ^1H NMR analysis of the titration of $[Mn(debpn)(H_2O)]^{2+}$ by EDTA. In this titration, 1 equiv. of EDTA quantitatively displaces the debpn ligand from the metal. In aqueous solution, water molecules may displace one or both of the debpn esters bound to the Mn(II), resulting in a mixture of species with $q = 1$, $q = 2$, or possibly even $q = 3$. Alternatively, transiently stable higher-coordinate species with $q = 2$ may form.[6] The solution data for the other metal complexes suggest that the debpn coordination is flexible enough to allow either of these mechanisms. Second, the rate of water exchange may be significantly different for $[Mn(debpn)(H_2O)]^{2+}$ and $[Mn(EDTA)(H_2O)]^{2-}$, which should result in different r_1 values for compounds with equal q values.[8] Third, the complexes may have substantially different interactions with outer-sphere water molecules. Given that EDTA should be able to more effectively hydrogen bond with water molecules than debpn, on the basis of its greater number of uncoordinated carbonyl groups, we find this third explanation unlikely.

The r_1 of 3.56 (±0.14) $mM^{-1}\ s^{-1}$ for $[Mn(debpn)(H_2O)]^{2+}$ compares favorably with values measured for Teslascan (2.8 $mM^{-1}\ s^{-1}$) and other mononuclear Mn(II)-containing contrast agents.[6,9,18,51] Direct comparisons are difficult, given the different conditions under which these complexes were analyzed and the paucity of theoretical work correlating the relaxitivities of manganese compounds with to such parameters. Five complexes recently reported by Wang and Westmoreland, for instances, were studied in water at 20 MHz.[6] The relaxitivity of the debpn complex also compares well to those of clinically relevant, mononuclear, Gd(III)-containing contrast agents, which generally have r_1 values of about 4 $mM^{-1}\ s^{-1}$.[11] The ability of $[Mn(debpn)(H_2O)]^{2+}$ to serve as a contrast agent is notable since the debpn ligand lacks both a macrocycle and an anionic charge, two features thought to be key to the stabilization of the aforementioned Mn(II) complexes in water.[7,8] The results may suggest that the design limitations for Mn(II) contrast agents may be more relaxed than previously thought and that other Mn(II) complexes with neutral, nonmacrocyclic ligands may also facilitate biological imaging.

The Mn(II) complex seems relatively robust. No hydrolysis of the ligand's ester groups is observed over 15 h in the HEPES buffer, as assessed by mass spectrometry. However, if the complex were to enter cells, esterases could potentially degrade the ligand. Other metal ions are capable of exchanging for the Mn(II) ion, but this exchange occurs slowly (Figure S6). When 1.0 mM $Fe(ClO_4)_2$ and 1.0 mM $[Mn(debpn)(H_2O)]^{2+}$ are allowed to react in MeCN, only 30% of the Mn(II) is displaced by the Fe(II) after 3 h. It should also be noted that physiological concentrations of chelatable metal ions are much lower than the 1.0 mM concentration of free iron used to achieve this modest rate of substitution.[52−55] Metal scavenging proteins and biomolecules may pose a more significant problem. EDTA, which may be thought of as a mimic of such species, quantitatively removes Mn(II) from the debpn complex.

The ability to use different sorts of Mn(II) complexes as imaging agents has potential clinical benefits. The positive charge of the $[Mn(debpn)(H_2O)]^{2+}$ complex may significantly alter its pharmacological properties relative to Teslascan, which is anionic. These properties include the sensor's abilities to permeate biological membranes and associate with particular tissues or cell types. Studies of the biological behavior of $[Mn(debpn)(H_2O)]^{2+}$ will explore these issues.

CONCLUSIONS

The novel ligand *N*,*N*′-bis(2-pyridylmethyl)-bis(ethylacetate)-1,2-ethanediamine (debpn) was found to chelate divalent first-row transition metal ions in both penta- and hexadentate

fashions. With larger first-row transition metal ions, the ligand is hexadentate, with an exogenous water molecule completing an overall pentagonal bipyramidal geometry. Despite the lack of a negative charge or a macrocycle within the debpn ligand's framework, the heptacoordinate Mn(II) complex with debpn can serve as a stable and effective MRI contrast agent under physiologically and clinically relevant conditions.

■ ASSOCIATED CONTENT

Supporting Information. Crystallographic data (CIF format), representative NMR and optical spectra (Figures S1–S5), least-squares analysis of debpn structures. This material is available free of charge via the Internet at http://pubs.acs.org.

■ AUTHOR INFORMATION

Corresponding Author
*E-mail: crgoldsmith@auburn.edu.

■ ACKNOWLEDGMENT

The authors thank Prof. Evert Duin for his assistance with the acquisition and interpretation of the EPR data and Dr. Michael Meadows for his assistance with the variable temperature NMR. This work was funded by Auburn University and a Doctoral New Investigator grant from the American Chemical Society- Petroleum Research Fund.

■ REFERENCES

(1) Casanova, D.; Alemany, P.; Bofill, J. M.; Alvarez, S. *Chem.—Eur. J.* **2003**, *9*, 1281–1295.
(2) Platas-Iglesias, C.; Vaiana, L.; Esteban-Gómez, D.; Avecilla, F.; Real, J. A.; de Blas, A.; Rodríguez-Blas, T. *Inorg. Chem.* **2005**, *44*, 9704–9713.
(3) Aston, K.; Rath, N.; Naik, A.; Slomczynska, U.; Schall, O. F.; Riley, D. P. *Inorg. Chem.* **2001**, *40*, 1779–1789.
(4) Summers, J. S.; Baker, J. B.; Meyerstein, D.; Mizrahi, A.; Zilbermann, I.; Cohen, H.; Wilson, C. M.; Jones, J. R. *J. Am. Chem. Soc.* **2008**, *130*, 1727–1734.
(5) Liu, G.-F.; Dürr, K.; Puchta, R.; Heinemann, F. W.; van Eldik, R.; Ivanović-Burmazović, I. *Dalton Trans.* **2009**, 6292–6295.
(6) Wang, S.; Westmoreland, T. D. *Inorg. Chem.* **2009**, *48*, 719–727.
(7) Troughton, J. S.; Greenfield, M. T.; Greenwood, J. M.; Dumas, S.; Wiethoff, A. J.; Wang, J.; Spiller, M.; McCurry, T. J.; Caravan, P. *Inorg. Chem.* **2004**, *43*, 6313–6323.
(8) Lauffer, R. B. *Chem. Rev.* **1987**, *87*, 901–927.
(9) Rocklage, S. M.; Cacheris, W. P.; Quay, S. C.; Hahn, F. E.; Raymond, K. N. *Inorg. Chem.* **1989**, *28*, 477–485.
(10) Oakes, J.; Smith, E. G. *J. Chem. Soc., Faraday Trans. 2* **1981**, *77*, 299–308.
(11) Caravan, P.; Ellison, J. J.; McMurry, T. J.; Lauffer, R. B. *Chem. Rev.* **1999**, *99*, 2293–2352.
(12) Caravan, P. *Acc. Chem. Res.* **2009**, *42*, 851–862.
(13) Thomsen, H. S. *Eur. Radiol.* **2004**, *14*, 1654–1656.
(14) Buhaescu, I.; Izzedine, H. *Int. J. Clin. Pract.* **2008**, *62*, 1113–1118.
(15) Kümmerer, K.; Helmers, E. *Environ. Sci. Technol.* **2000**, *34*, 573–577.
(16) Mukhopadhyay, S.; Mandal, S. K.; Bhaduri, S.; Armstrong, W. H. *Chem. Rev.* **2004**, *104*, 3981–4026.
(17) Wieghardt, K. *Angew. Chem., Int. Ed.* **1989**, *28*, 1153–1172.
(18) Schwert, D. D.; Davies, J. A.; Richardson, N. *Top. Curr. Chem.* **2002**, *221*, 165–199.
(19) Drew, M. G. B.; bin Othman, A. H.; McFall, S. G.; McIlroy, P. D. A.; Nelson, S. M. *J. Chem. Soc., Dalton Trans.* **1977**, 1173–1180.
(20) Seitz, M.; Kaiser, A.; Stempfhuber, S.; Zabel, M.; Reiser, O. *Inorg. Chem.* **2005**, *44*, 4630–4636.
(21) Hulsbergen, F. B.; Driessen, W. L.; Reedijk, J.; Verschoor, G. C. *Inorg. Chem.* **1984**, *23*, 3588–3592.
(22) Hoard, J. L.; Pedersen, B.; Richards, S.; Silverton, J. V. *J. Am. Chem. Soc.* **1961**, *83*, 3533–3534.
(23) Zetter, M. S.; Grant, M. W.; Wood, E. J.; Dodgen, H. W.; Hunt, J. P. *Inorg. Chem.* **1972**, *11*, 2701–2706.
(24) El Ghachtouli, S.; Mohamadou, A.; Barbier, J.-P. *Inorg. Chim. Acta* **2005**, *358*, 3873–3880.
(25) Haynes, J. S.; Sams, J. R.; Thompson, R. C. *Can. J. Chem.* **1981**, *59*, 669–678.
(26) Toftlund, H.; Pedersen, E.; Yde-Andersen, S. *Acta. Chem. Scand. A* **1984**, *38*, 693–697.
(27) Bernstein, M. A.; King, K. F.; Zhou, X. J. *Handbook of MRI Pulse Sequences*; Elsevier Academic Press: Amsterdam, 2004.
(28) Haacke, E. M.; Brown, R. W.; Thompson, M. R.; Venkatesan, R. *Magnetic Resonance Imaging: Physical Principles and Sequence Design*; John Wiley & Sons: New York, NY, 1999.
(29) Nelder, J. A.; Mead, R. *Comput. J.* **1965**, *7*, 308–313.
(30) Britovsek, G. J. P.; England, J.; White, A. J. P. *Dalton Trans.* **2006**, 1399–1408.
(31) Shannon, R. D. *Acta Crystallogr.* **1976**, *A32*, 751–767.
(32) Coates, C. M.; Hagan, K.; Mitchell, C. A.; Gorden, J. D.; Goldsmith, C. R. *Dalton Trans.* **2011**, *40*, 4048–4058.
(33) Costas, M.; Que, L., Jr. *Angew. Chem., Int. Ed.* **2002**, *41*, 2179–2181.
(34) Coates, C. M.; Nelson, A.-G. D.; Goldsmith, C. R. *Inorg. Chim. Acta* **2009**, *362*, 4797–4803.
(35) Goldsmith, C. R.; Cole, A. P.; Stack, T. D. P. *J. Am. Chem. Soc.* **2005**, *127*, 9904–9912.
(36) Dowsing, R. D.; Gibson, J. F.; Goodgame, M.; Hayward, P. J. *J. Chem. Soc. A* **1969**, 187–193.
(37) Gosiewska, S.; Cornelissen, J. J. L. M.; Lutz, M.; Spek, A. L.; van Koten, G.; Klein Gebbink, R. J. M. *Inorg. Chem.* **2006**, *45*, 4214–4227.
(38) Klein Gebbink, R. J. M.; Jonas, R. T.; Goldsmith, C. R.; Stack, T. D. P. *Inorg. Chem.* **2002**, *41*, 4633–4641.
(39) Drago, R. S. *Physical Methods for Chemists*, 2 ed.; Surfside Scientific Publishers: Gainesville, FL, 1992.
(40) Brown, M. A.; Johnson, G. A. *Med. Phys.* **1984**, *11*, 67–72.
(41) Bandara, H. M. D.; Kennedy, D. P.; Akin, E.; Incarvito, C. D.; Burdette, S. C. *Inorg. Chem.* **2009**, *48*, 8445–8455.
(42) Glerup, J.; Goodson, P. A.; Hodgson, D. J.; Michelsen, K. *Inorg. Chem.* **1995**, *34*, 6255–6264.
(43) Maigut, J.; Meier, R.; Zahl, A.; van Eldik, R. *J. Am. Chem. Soc.* **2008**, *130*, 14556–14569.
(44) Buschhaus, B.; Hampel, F.; Grimme, S.; Hirsch, A. *Chem.—Eur. J.* **2005**, *11*, 3530–3540.
(45) López-Deber, M.; Bastida de la Calle, R.; Macías, A.; Pérez-Lourido, P.; Rodríguez, A.; Valencia Matarranz, L. *Z. Anorg. Allg. Chem.* **2007**, *633*, 1842–1846.
(46) Waynant, K. V.; White, J. D.; Zakharov, L. *Chem. Commun.* **2010**, *46*, 5304–5306.
(47) March, R.; Clegg, W.; Coxall, R. A.; González-Duarte, P. *Inorg. Chim. Acta* **2003**, *346*, 87–94.
(48) Singh, G.; Sowerby, D. B. *J. Chem. Soc., Dalton Trans.* **1977**, 490–492.
(49) Kang, S.-G.; Kweon, J. K.; Jeong, J. H. *Inorg. Chim. Acta* **2007**, *360*, 1875–1882.
(50) Zhou, M.; Andrews, L.; Bauschlicher, C. W., Jr. *Chem. Rev.* **2001**, *101*, 1931–1962.
(51) Elizondo, G.; Fretz, C. J.; Stark, D. D.; Rocklage, S. M.; Quay, S. C.; Worah, D.; Tsang, Y.-M.; Chen, M. C.; Ferrucci, J. T. *Radiology* **1991**, *178*, 73–78.
(52) Outten, C. E.; O'Halloran, T. V. *Science* **2001**, *292*, 2488–2492.
(53) Theil, E. C.; Goss, D. J. *Chem. Rev.* **2009**, *109*, 4568–4579.
(54) Zhang, Y.; Gladyshev, V. N. *Chem. Rev.* **2009**, *109*, 4828–4861.
(55) Ba, L. A.; Doering, M.; Burkholz, T.; Jacob, C. *Metallomics* **2009**, *1*, 292–311.